

Locating active-site hydrogen atoms in D-xylose isomerase: Time-of-flight neutron diffraction

Amy K. Katz^{†‡}, Xinmin Li[‡], H. L. Carrell[†], B. Leif Hanson[§], Paul Langan[¶], Leighton Coates[¶], Benno P. Schoenborn[¶], Jenny P. Glusker[†], and Gerard J. Bunick^{||†‡‡‡}

[†]Fox Chase Cancer Center, 333 Cottman Avenue, Philadelphia, PA 19111; [‡]Graduate School of Genome Science and Technology, University of Tennessee, F337 Walters Life Science Building, 1414 West Cumberland Avenue, Knoxville, TN 37996; [§]Instrumentation Center, 2801 West Bancroft M/S 602, University of Toledo, Toledo, OH 43606; [¶]Bioscience Division, Los Alamos National Laboratory, M888, Life Science Division, Los Alamos, NM 87545; ^{||}Graduate School of Genome Science and Technology, University of Tennessee, 1060 Commerce Park Drive, Oak Ridge, TN 37830; and ^{†††}Department of Biochemistry, Cellular, and Molecular Biology and the Center of Excellence for Structural Biology, University of Tennessee, Walters Life Science Building F337, Knoxville, TN 37996

Communicated by Jane S. Richardson, Duke University Medical Center, Durham, NC, March 30, 2006 (received for review November 3, 2005)

Time-of-flight neutron diffraction has been used to locate hydrogen atoms that define the ionization states of amino acids in crystals of D-xylose isomerase. This enzyme, from *Streptomyces rubiginosus*, is one of the largest enzymes studied to date at high resolution (1.8 Å) by this method. We have determined the position and orientation of a metal ion-bound water molecule that is located in the active site of the enzyme; this water has been thought to be involved in the isomerization step in which D-xylose is converted to D-xylulose or D-glucose to D-fructose. It is shown to be water (rather than a hydroxyl group) under the conditions of measurement (pH 8.0). Our analyses also reveal that one lysine probably has an $-NH_2$ -terminal group (rather than NH_3^+). The ionization state of each histidine residue also was determined. High-resolution x-ray studies (at 0.94 Å) indicate disorder in some side chains when a truncated substrate is bound and suggest how some side chains might move during catalysis. This combination of time-of-flight neutron diffraction and x-ray diffraction can contribute greatly to the elucidation of enzyme mechanisms.

amino acid ionization states | enzyme mechanism | x-ray diffraction | deuterium/hydrogen in proteins | proton transfer

The enzyme D-xylose isomerase (XI) from the bacterium *Streptomyces rubiginosus*, a homotetramer of molecular mass 173 kDa, is one of a large class of aldose–ketose isomerases that require two divalent metal ions for function. The folding of its backbone, that of a $(\beta\alpha)_8$ barrel, was first determined by us in 1984 (1). We report here our structural studies by time-of-flight neutron diffraction; XI is among the largest enzymes studied by this method. One metal ion (M1) binds four carboxylate groups (Glu-181, Glu-217, Asp-245, and Asp-287) and two water molecules (W1116 and W1218 in Fig. 1). The substrate binds at this site, displacing the two metal-bound water molecules. The other metal site (M2) binds three carboxylate groups (Glu-217, Asp-257, and bidentate Asp-255), one water molecule, and a His residue (His-220). The carboxylate group of Glu-217 is shared by both metal ions.

XI catalyzes the interconversion of the aldo-sugars D-xylose or D-glucose to the keto-sugars D-xylulose and D-fructose, respectively. There are two sites in XI where hydrogen transfer is involved in a catalytic mechanism. One involves the opening of the ring of the cyclic sugar substrate to give a straight-chain sugar that the enzyme then can isomerize. This ring-opening takes place near one of the metal ions, M1 (in the upper region of Fig. 1), and involves His-54 (2, 3). The second region is the site of the isomerization of an aldose to ketose, that is, where the transfer of a hydrogen atom between adjacent carbon atoms on the substrate occurs. This site is somewhat nearer to M2 (the lower left region of Fig. 1). Three possible mechanisms involving a *cis*-ene diol intermediate, a hydride shift, or a metal-mediated hydride shift have been suggested (see figure 1 of ref. 4). To establish hydrogen (deuterium) atom locations in this enzyme, neutron diffraction studies were initiated.

The transfer of hydrogen or hydride ions in the active site is commonly found in many enzyme reaction mechanisms. These hydrogen atoms or ions are, however, difficult to locate. Structural studies by x-ray diffraction, even to resolutions better than 1 Å (5–7), may not provide their locations. In an x-ray analysis of aldose reductase at the extremely high resolution of 0.66 Å, Podjarny and coworkers (7) noted that only 54% of all hydrogen atoms could be located (77% of hydrogen atoms in the active site). There are two main reasons for this problem. First, the amount of x-ray scattering of an atom depends on its atomic number, and hydrogen, with the lowest atomic number, 1, is a very poor scatterer of x-rays. Secondly, transferable hydrogen atoms in a biological macromolecule may be mobile and therefore in different positions in different unit cells in the crystal. As a result, their electron densities are distributed over a larger volume. Commonly used procedures for defining hydrogen atom positions are to predict them from the known geometries of certain functional groups and from their inferred positions in suggested hydrogen-bonding patterns (8, 9). These methods do not, however, unequivocally establish hydrogen atom locations; they only provide an educated guess as to where they might be.

This problem of locating hydrogen atoms in proteins, however, has been successfully addressed by neutron studies (10, 11), because the neutron scattering power of an atom, unlike that for x-ray scattering, does not depend directly on its atomic number (www.ncnr.nist.gov/resources/n-lengths). Deuterium (atomic weight 2, neutron scattering length $+6.67 \times 10^{-15}$ m) (11) scatters to the same extent as carbon and oxygen ($+6.65$ and $+5.80 \times 10^{-15}$ m, respectively) (11) and gives a good positive peak in the neutron-density (nuclear-density) map. These peaks can be seen clearly in maps at the relatively medium resolution of ≈ 2 Å, even when they cannot always be located with certainty in a 0.66-Å x-ray study (7, 12, 13). The other common isotope, hydrogen itself (atomic weight 1, neutron scattering length -3.74×10^{-15} m) (11) gives a negative peak in a nuclear-density map. These scattering properties provide a method for locating hydrogen atoms (by introducing deuterium into the macromolecule) and for identifying which hydrogen atoms are readily replaced by deuterium and the extent of this replacement (by estimating the approximate proportion of the two isotopes of hydrogen at each site from examination of the peak height in the nuclear-density map). Thus, neutron diffraction studies provide two items that are hard or impossible to obtain from macromolecular x-ray diffraction studies: the locations of hydrogen atoms, often including the more mobile ones, and the extent to which

Conflict of interest statement: No conflicts declared.

Abbreviations: XI, D-xylose isomerase; PDB, Protein Data Bank.

Data deposition: The atomic coordinates and structure factors have been deposited in the Protein Data Bank, www.pdb.org (PDB ID codes 2GLK, 2GUB, and 2GVE).

^{††}To whom correspondence should be addressed. E-mail: gjbunick@utk.edu.

© 2006 by The National Academy of Sciences of the USA

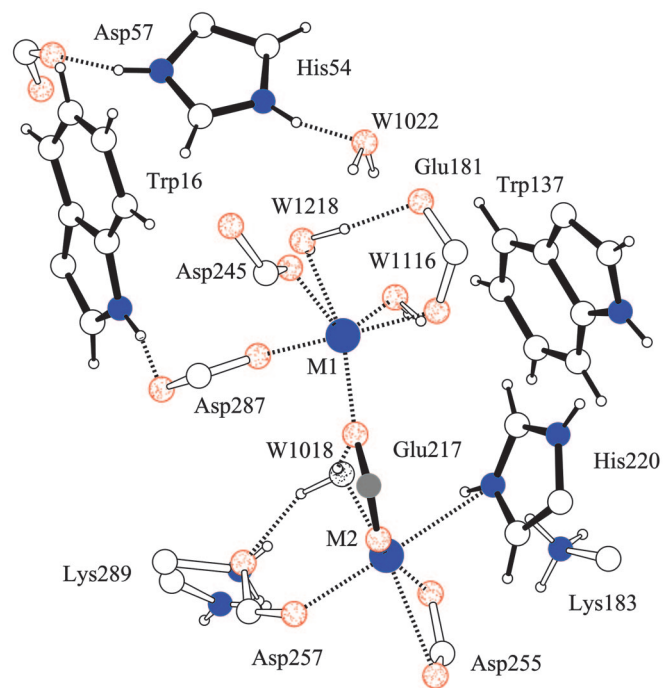


Fig. 1. Active site of XI showing most of the amino acid residues described in this work. The two Trp and two His residues that define the “box” are drawn with black-filled bonds, as is Glu-217, which is shared by both metal ions, M1 and M2.

a particular hydrogen atom can be replaced by deuterium (that is, its chemical reactivity and its accessibility to exchange reactions).

One significant outcome is that, by neutron diffraction, it is possible to determine whether an amino acid side chain in a protein is ionized or not. A result is that analyses as a function of pH are possible and additional information relevant to possible enzyme mechanisms can be obtained in this way. The amino acid side chain that is most amenable to manipulation with respect to protonation state near neutral pH is His. Acid side chains (Asp and Glu) are generally ionized at this pH, but the usefulness of information on their C—O bond lengths (equal for carboxylates, unequal for nonionized acids) depends on the resolution and how independently the C and O atoms were refined.

The usefulness of neutron diffraction was demonstrated in a study of the mechanism of action of a Ser protease. This result was established by x-ray diffraction and biochemical investigations (14–16), followed by a neutron-diffraction study, as reported by Kossiakoff and Spencer (14) several years ago. The protonation states of His-57, Asp-102, and Ser-195 were determined by neutron-diffraction studies of the deuterated bovine enzyme inhibited by a transition-state analogue at a pH near 7. These studies showed (at 2.2-Å resolution) that there were two nitrogen-bound deuterium atoms on His-57 and none on Asp-102. Thus, it could be inferred that the function of Asp-102 is to stabilize the imidazolium protonation state of His-57 (14–18).

We present here the results of neutron-diffraction studies on the enzyme XI from *S. rubiginosus*, with particular emphasis on the protonation states of His, Lys, and water. We will describe the positions of the deuterons located on His-54, His-220, Lys-289, and an important water molecule and comment on the significance of the result to our understanding of the mechanism of this enzyme.

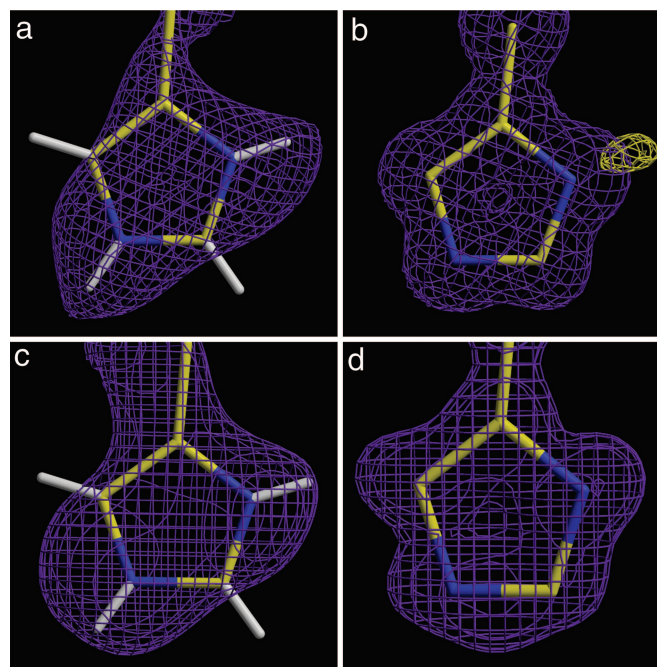


Fig. 2. Doubly protonated His residues in $2F_o - F_c$ nuclear-density maps (1.8-Å resolution) (a and c) and $2F_o - F_c$ electron-density maps (0.94 Å resolution) (b and d) for His-54 (a and b) and His-220 (c and d). In a, both ring nitrogen atoms, ND1 and NE2, are protonated. The difference electron density ($F_o - F_c$, gold) in b confirms that His-54 ND1 is protonated, but there is no indication of a proton on the other ring nitrogen atom, NE2. In c, the nuclear density for His-220 reveals that ND1 and NE2 are both protonated. The protonation state of ND1 and NE2 cannot be unambiguously determined from the electron density for His-220 in d but is clear in c.

Results and Discussion

The active site of this enzyme is shaped like a shoebox (see Fig. 1) with two Trp residues (Trp-16 and -137) on opposite sides. They serve as hydrophobic restraints and control the width of the sugar-binding pocket and hence the size of a substrate. At the two ends of the box are His residues, His-54, which acts to open the ring of the newly bound substrate, and His-220, which plays a role in the subsequent isomerization at the other end of the substrate molecule (top and bottom of Fig. 1, respectively). These amino acid residues control the length of the substrate. In addition, His-220 controls the electrostatics of the C2—O2 bond of the substrate (via the proton on CE1 of His-220) (19, 20).

Our observations with respect to the mechanism of the enzyme were from several electron-density maps and one nuclear-density map. The electron-density maps (from x-ray studies) consist of a high-resolution map of the enzyme with bound glycerol (designated UHR; resolution 0.94 Å; low temperature, 100 K; G.J.B., H.L.C., B.L.H., A.K.K., and J.P.G., unpublished data), the enzyme with bound substrate xylulose [Protein Data Bank (PDB) ID code 1XII] or glucose (PDB ID code 1XIF) (21), and the metal-free enzyme (H.L.C., A.K.K., and J.P.G., unpublished data).

The presence of glycerol in the UHR analysis has greatly aided our study. It provided a “stunted substrate” that apparently could trigger a binding signal (near M1), but had no atoms that could bind in the isomerization area of the active site. As a result, we were able to detect motions of the amino acid residues that would be expected to interact with a longer bound molecule (an active substrate, for example). The UHR electron-density map showed that several side chains, specifically Glu-181, Glu-186, Asp-255, and Asp 257, are flexible and in different positions from unit cell to unit cell.

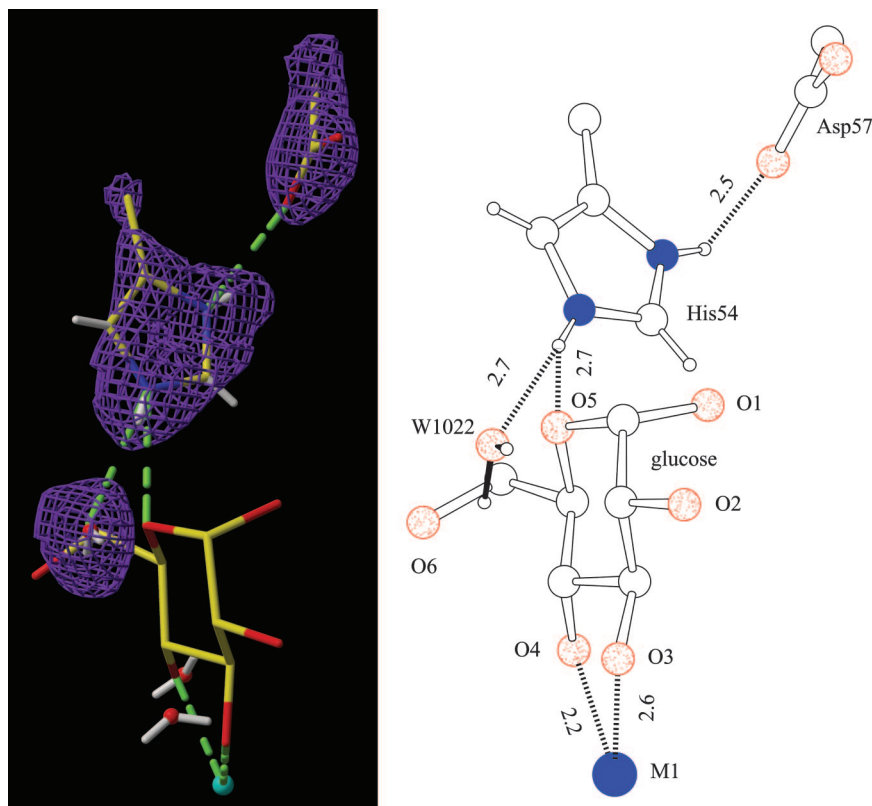


Fig. 3. Spatial relationship of glucose substrate to His-54. (*Left*) Neutron map (1.8-Å resolution) showing His-54 with coordinates of glucose from an x-ray study (1.6-Å resolution; PDB ID code 1XIF) shown by yellow lines. Nuclear density is shown for Asp-57, His-54, and heavy water W1022. (*Right*) Model with W1022 superimposed on the site of a metal ion-bound cyclic glucose. His-54 NE2 provides a proton to the water molecule (W1022 at 2.67 Å) in the absence of substrate. Presumably, when the cyclic form of the sugar substrate is present, the water molecule is displaced, and a hydrogen bond (2.68 Å) is formed between His-54 NE2 and O5 of the sugar. This result shows a possible mode of protonation required for substrate ring opening. The metal ion, M1, that binds the other end of the cyclic glucose, is shown at the bottom of the diagrams.

Nuclear-density maps at 1.8 Å showed that all aspartic and glutamic acid side chains, at the pH of measurement (pH 8.0), were ionized; each lacked an attached proton. These maps gave especially good information on the nitrogen-containing side chains because the scattering power of nitrogen for neutrons (9.36×10^{-15} m) is higher than that for oxygen, carbon, or deuterium (11). Several of the His side chains were doubly protonated in the neutron crystal structure, as shown by the two examples in Fig. 2. All 10 His residues have been examined and placed into one of two groups, singly (His-49, -71, -96, and -243) or doubly protonated (His-54, -198, -220, -230, -285, and -382). Of the singly protonated His residues, the H/D is on ND1 for His-49 and -243, and on NE2 for His-71 and -243. The ratio of deuterium to hydrogen was determined from H/D occupancy refinement and peak height measurements. Because, to substitute the deuterium for hydrogen, it is necessary to break the N-H bond, these values give an indication of the strength of an N-H bond and how accessible it is to exchange with D₂O. The stronger and/or less accessible a bond, the lower the percentage of hydrogen-to-deuterium exchange.

Our neutron-diffraction analysis showed that His-54 (which is doubly protonated) provides a proton to a water molecule (W1022) in the absence of substrate. This water molecule is displaced when the cyclic form of the sugar substrate is bound. A comparison (see Fig. 3) was made of the UHR x-ray crystal structure, which contains this water, the structure with bound cyclic glucose (PDB ID code 1XIF; x-ray structure at 1.6-Å resolution; ref. 21), and the current neutron structure. These are approximately isomorphous, except in the area of bound ligand.

The comparison showed that W1022, which is hydrogen bonded to an NH group of His-54, lies very near the position of the ring oxygen of glucose in the 1XIF study (Fig. 3). This result implies that His-54 forms an N-H...O hydrogen bond to the ring oxygen of glucose, thereby aiding the ring opening. Few other demonstrations of the possible geometry of proton transfer during ring opening have been described. Furthermore the 1XIF-enzyme-glucose crystal structure shows that, compared with the structure with xylulose in place of glucose (1XII; ref. 21), the longer glucose molecule positions its additional CH₂OH group (C6) in a direction away from the two metal sites (Fig. 4). Thus, the extra length of glucose (compared with xylose) projects into an area that is not involved with the active site.

The successful binding of a cyclic substrate is detected both by Glu-181 (OE1 interacting with O4 of glucose and OE2 interacting with M1) and by His-220 (CE1 interacting with both OE2 of Glu-181 and O3 of glucose) (Fig. 4a). When the sugar ring is opened, O4 stays in place, bound to the metal ion, whereas O3 moves toward the hydrophobic surface of Trp-16 (Fig. 4b). Lys-183 then interacts with O1 of the substrate (see Fig. 4b). The C-H group (CE1) of His-220 now interacts with O2 in the linear substrate (a hydroxyl group in xylose, a carbonyl group in the product, xylulose).

His-220 in the active site is doubly protonated ≈50% of the time. This finding was a surprise to us because the identified His NH group had been thought to be bound to the metal ion (M2). In the neutron analysis the metal ions, cobalt and manganese, are both present, but their scattering powers (bound coherent scattering lengths, Co, 2.49×10^{-15} m; Mn, -3.73×10^{-15} m)

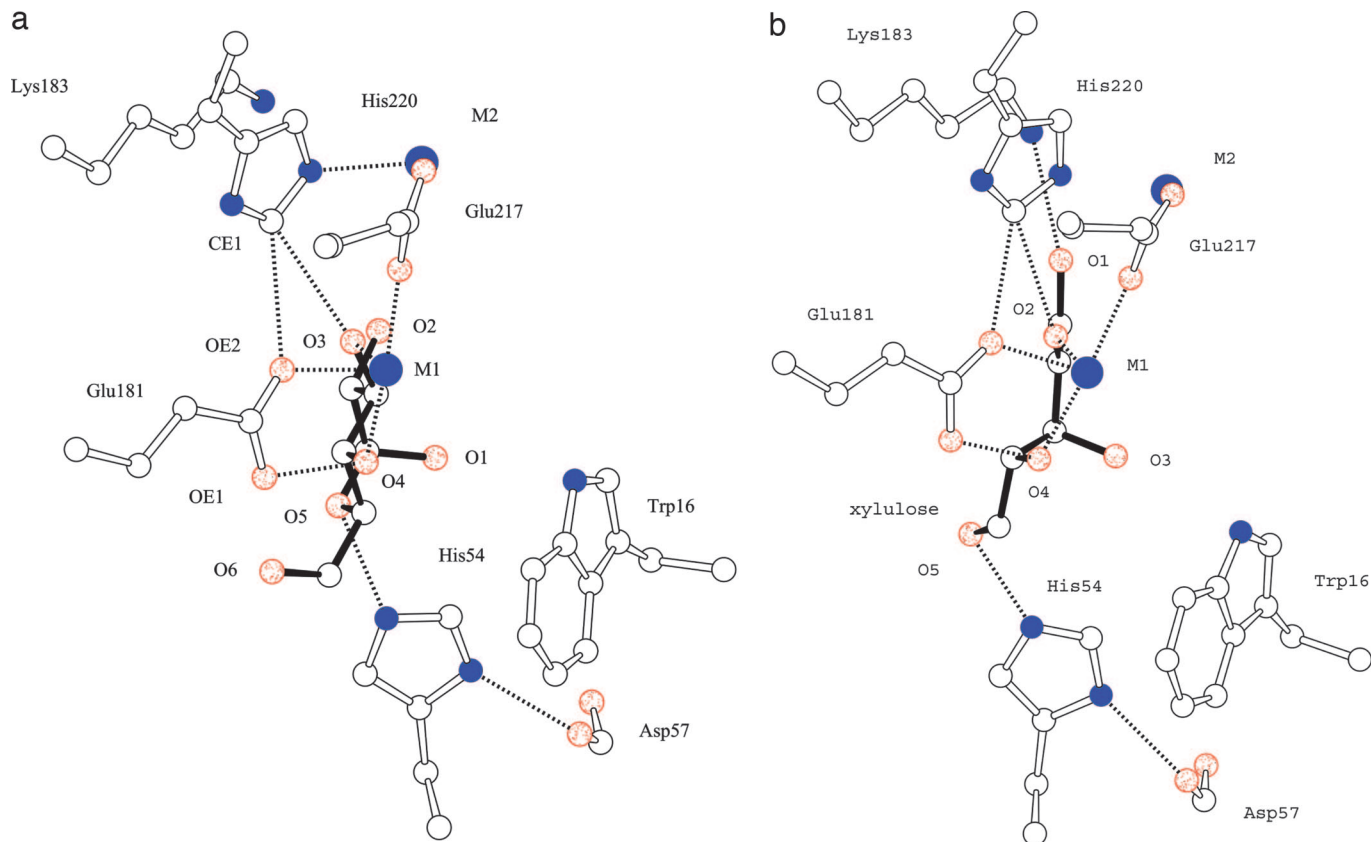


Fig. 4. Comparison of the binding of glucose (substrate) and xylulose (product). (a) The detection and binding of a cyclic substrate (glucose) is detailed. (b) Diagram of the binding arrangement for linear xylulose. Note that the additional CH₂OH group (C6) of the longer glucose molecule (as compared with xylose) projects into an area that is not involved with the isomerization area of the active site. The movement of Lys-183 associated with the formation a hydrogen bond to O1 of the linear form of the substrate is shown. The two views are drawn in the same orientation.

cancel each other out (11). We have, however, determined the x-ray crystal structure of the metal-free enzyme and so know which groups move to fill the voids left by the cations. In the

current neutron structure, these groups are arranged as in the metal ion-containing enzyme, not the metal-free enzyme. It is clear that His-220 is not tightly bound to the metal ion, and its

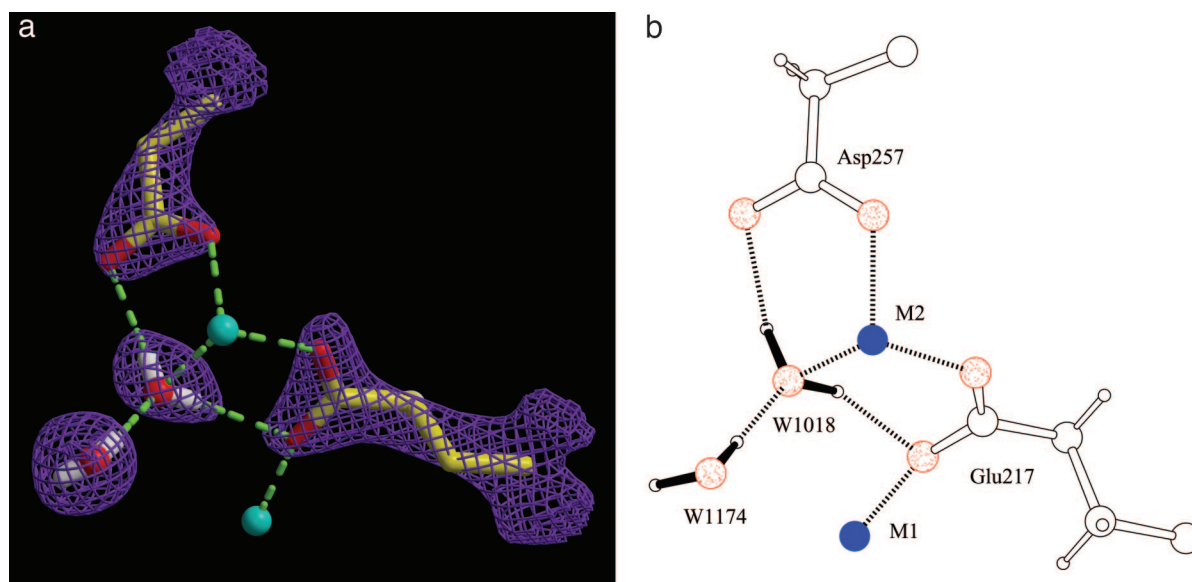


Fig. 5. Environment of proposed catalytic water (shown with heavy black bonds). (a) Nuclear density ($2F_o - F_c$). (b) Atomic arrangement in the 1.8-Å-resolution neutron map. Both diagrams show the water molecule (with an elongated shape indicating two protons) and the two metal ion-carboxylate-water motifs. In the electron-density map (data not shown), two possible conformations exist for Asp-257, one of which agrees with the nuclear-density results shown here.

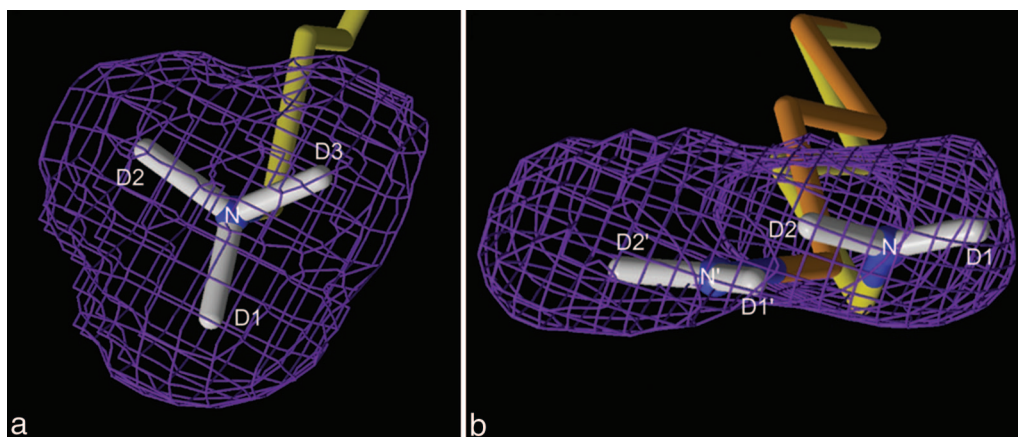


Fig. 6. Surroundings of Lys-183 (a) and Lys-289 (b) in the nuclear-density map. Lys-289 adopts two conformations in this map. Note that each of the conformers of Lys-289 only has two protons, whereas Lys-183 has three. In the UHR electron-density map, NZ is rotated $\approx 88^\circ$ counterclockwise from the yellow conformation in *b*. This rotation brings NZ to within 2.74 Å of one of the two conformers of Asp-257. Rotation about the Lys-289 CE–NZ bond is not sterically restricted in either the x-ray or neutron structures.

position indicates that it is leaving this coordination site. The neutron study shows that the deuterium on NE2 of His-220 is pointing toward OD2 of Asp-255 when the aspartic acid is in its conformation furthest from the metal ion. This result indicates how His-220 would move when it leaves the metal ion.

We initiated this neutron diffraction study of XI to find out whether the catalytic “water” molecule (W1018) is truly water or whether it has been ionized to a hydroxyl group. As shown in Fig. 5*a*, we found that it is, indeed, a water molecule. It is, of course, possible that this water molecule might become ionized to a hydroxyl group, but the structure determination was carried out at a somewhat alkaline pH (8.0). W1018 is bound to M2 in the x-ray structure and takes part in two metal ion–carboxylate–water motifs (22) involving a carboxylate (Asp-257 and Glu-217) and M2, diagrammed in Fig. 5*b*. These two deuterium atoms, clearly visible in the nuclear-density map (Fig. 5*a*), each take part in a motif that would strongly orient the two lone pairs of the water oxygen atom in specific directions. The nuclear-density map indicates that the oxygen atom of W1018 points one of its lone pair of electrons toward the metal ion and the other toward the active site C–C bond of the substrate. Thus, this lone pair of electrons from W1018 might be the proton-abstracting group required for the second stage of the enzyme reaction mechanism (rather than a hydride shift). Because Asp-257 is hydrogen bonded to W1018 it may be able to abstract a hydrogen from this water molecule if it has been sufficiently polarized by the metal ion (Fig. 5).

Another significant finding in the neutron study is that Lys-289 appears to have only two deuterium (hydrogen) atoms bound to it, not the expected three. A comparison of this Lys residue with Lys-183, is shown in Fig. 6. To our knowledge, a direct observation of a Lys NH_2 group in an enzyme has not been previously described. All other Lys residues are fully protonated. Also of importance is the finding from the nuclear-density map that Lys-289 adopts multiple conformations. Examination of the proximity of NZ reveals that it can swing about by rotation of the CE–NZ bond. This amino acid residue is more visible in the nuclear density than in the UHR electron-density map. The determination that Lys-289 probably has only two protons, and its proximity to Asp-257 suggests that it could accept a proton from the aspartic acid (for example, a proton originating on W1018). Lys-289 could move to accept this proton as Asp-257 moves to deliver it. NZ of Lys-183 has three binding partners, a water molecule, the main-chain carbonyl group of Glu-186, and the carboxylate group of either Glu-186 or Asp-255.

Which of these two residues accepts the third hydrogen bond from Lys-183 depends on how well Asp-255 is bound to the metal.

This neutron structure analysis has provided some unexpected results, and, if crystals of a suitable size can be obtained, this type of study is recommended for other enzymes. We have demonstrated the presence of water (D_2O) rather than a hydroxyl group bound to the metal ion at the site of the isomerization reaction, the lack of a third proton on Lys-289, and the tendency for His-220 (partially protonated at NE2) to leave its metal-binding site. These findings were possible because deuterium atoms could be confidently located in nuclear-density maps. They demonstrate that combined neutron and x-ray diffraction studies provide a powerful methodology for elucidating enzyme mechanisms.

Methods

Sample Preparation. The enzyme XI used for crystallization was purified from a stock solution of commercial food-grade product (Gensweet SGI; kindly provided by Genencor International, Palo Alto, CA). Two counterdiffusion dialysis devices were used in the crystallization of XI for neutron analysis, the diffusion-controlled apparatus for microgravity (DCAM) and the counterdiffusion cell (CDC). The growth of near-perfect crystals >2 mm in each direction required ≈ 3 months. The counterdiffusion cells also were used for gradually exchanging the crystallization solutions to deuterated components before diffraction experiments (4, 23). Descriptions of sample preparation and crystallization are in ref. 4.

Data Collection and Processing. The room-temperature (20°C) neutron diffraction data were measured at the Protein Crystallography Station (PCS) at the Los Alamos Neutron Science Center. A kappa circle goniometer was used as described in ref. 4. The exposure time at each crystal setting was typically 12–20 h. The quality of the data, indicated by the number of strongly measured reflections, was proportional to the exposure time. Data collection strategies on the PCS are described in greater detail by Langan and Greene (24). Data indexing and integration was performed by using a version of D^*TREK that had been modified for wavelength-resolved Laue neutron protein crystallography, which is described in further detail by Pflugrath (25) and Langan and Greene (26). An automatic-peak finding routine located between 500 and 1,000 strong peaks ($d > 1.8$ Å) at each crystal setting. These peaks were used to determine the crystal orientation matrix. The total number of integrated reflections from the crystal was 221,268, of which 32,390 were unique with

$d > 1.8 \text{ \AA}$. After integration, the data were converted into a format for input into the program LAUENORM (27). Using the data from all crystal settings, six iterations of a combined five cycles of wavelength normalization and four cycles of intercycle scaling were performed. The wavelength normalization curve was modeled by using nine Chebyshev polynomials (28). To obtain reasonable values for R_{merge} , the wavelength range was restricted to 0.9–6.5 \AA , and only reflections with $I > 3\sigma$ were used in determining the wavelength normalization polynomial. The LAUENORM data were output in unmerged form so that SCALA (29) could be used for statistical analysis. Only data with $I/\sigma(I) > 1.5$ were used in data scaling. For additional details on data processing, see ref. 4.

Structure Solution and Refinement. Molecular refinement of the neutron diffraction data was initiated by using atomic positions of the atoms determined from our 1.60- \AA -resolution x-ray

structure (PDB ID code 1XIB with water molecules removed) (30). Models were fit and refined by using the computer programs XTALVIEW and SHELX, respectively (31, 32). These 1.8- \AA -resolution nuclear-density maps contained protein plus water and metal ions but no substrate or inhibitor. Three-dimensional coordinates of the three structures described here have been deposited in the Protein Data Bank (30).

We thank Dr. Joel M. Harp for his contributions to the research. Parts of this work were supported by National Institutes of Health Grants GM-29818 (to G.J.B.), CA-10925 (to J.P.G.), and CA-06927 (to Fox Chase Cancer Center). G.J.B. was supported by the Oak Ridge National Laboratory Director's Research and Development seed money and National Aeronautics and Space Administration Grants NAG8-1568 and NAG8-1826. The Protein Crystallography Station is supported by the Office of Science and the Office of Biological and Environmental Research of the U.S. Department of Energy.

- Carrell, H. L., Rubin, B. H., Hurley, T. J. & Glusker, J. P. (1984) *J. Biol. Chem.* **259**, 3230–3236.
- Collyer, C. A., Henrick, K. & Blow, D. M. (1990) *J. Mol. Biol.* **212**, 211–235.
- Collyer, C. A. & Blow, D. M. (1990) *Proc. Natl. Acad. Sci. USA* **87**, 1362–1366.
- Hanson, B. L., Langan, P., Katz, A. K., Li, X., Harp, J. M., Glusker, J. P., Schoenborn, B. P. & Bunick, G. J. (2004) *Acta Crystallogr. D* **60**, 241–249.
- Niimura, N., Mizuno, H., Helliwell, J. R. & Westhof, E., eds. (2005) *Hydrogen- and Hydration-Sensitive Structural Biology* (KubaPro, Tokyo).
- Coates, L. & Myles, D. A. A. (2004) *Curr. Drug Targets* **5**, 173–178.
- Howard, E. I., Sanishvili, R., Cachau, R. E., Mitschler, A., Chevrier, B., Barth, P., Lamour, V., Van Zandt, M., Sibley, E., Bon, C., et al. (2004) *Proteins Struct. Funct. Bioinform.* **55**, 792–804.
- Lovell, S. C., Davis, I. W., Arendall, W. B., III, de Bakker, P. I. W., Word, J. M., Prisant, M. G., Richardson, J. S. & Richardson, D. C. (2003) *Proteins Struct. Funct. Genet.* **50**, 437–450.
- McDonald, I. K. & Thornton, J. M. (1994) *J. Mol. Biol.* **238**, 777–793.
- Bacon, G. E. (1975) *Neutron Diffraction* (Oxford Univ. Press, Oxford), 3rd Ed.
- Sears, V. F. (1992) *Neutron News* **3** (3), 29–37.
- Ko, T.-P., Robinson, H., Gao, Y.-G., Cheng, C.-H. C., Devries, A. L. & Wang, A. H.-J. (2003) *Biophys. J.* **84**, 1228–1237.
- Jelsch, C., Teeter, M. M., Lamzin, V., Pichon-Pesme, V., Blessing, R. H. & Lecomte, C. (2000) *Proc. Natl. Acad. Sci. USA* **97**, 3171–3176.
- Kossiakoff, A. A. & Spencer, S. A. (1981) *Biochemistry* **20**, 6462–6474.
- Bachovchin, W. W. (1985) *Proc. Natl. Acad. Sci. USA* **82**, 7948–7951.
- Carter, P. & Wells, J. A. (1988) *Nature* **332**, 564–568.
- Craik, C. S., Rocznik, S., Largman, C. & Rutter, W. J. (1987) *Science* **237**, 909–913.
- Voet, D., Voet, G. J. & Pratt, C. W. (1999) *Fundamentals of Biochemistry* (Wiley, New York).
- Derewenda, Z. S., Derewenda, U. & Kobos, P. M. (1994) *J. Mol. Biol.* **241**, 83–93.
- Hedstrom, L. (2002) *Chem. Rev.* **102**, 4501–4524.
- Carrell, H. L., Hoier, H. & Glusker, J. P. (1994) *Acta Crystallogr. D* **50**, 113–123.
- Kaufman, A., Afshar, C., Rossi, M., Zacharias, D. E. & Glusker, J. P. (1993) *Struct. Chem.* **4**, 191–198.
- Carter, D. C., Wright, B., Miller, T., Chapman, J., Twigg, P., Keeling, K., Moody, K., White, M., Click, J., Ruble, J., et al. (1999) *J. Cryst. Growth* **196**, 602–609.
- Langan, P. & Greene, G. (2004) *J. Appl. Cryst.* **37**, 253–257.
- Pflugrath, J. W. (1999) *Acta Crystallogr. D* **55**, 1718–1725.
- Langan, P., Greene, G. & Schoenborn, B. P. (2004) *J. Appl. Cryst.* **37**, 24–31.
- Helliwell, J. R., Habash, J., Cruickshank, D. W. J., Harding, M. M., Greenhough, T. J., Campbell, J. W., Clifton, I. J., Elder, M., Machin, P. A., Papiz, M. Z. & Zurek, S. (1989) *J. Appl. Cryst.* **22**, 483–497.
- Arzt, S., Campbell, J. W., Harding, M. M., Hao, Q. & Helliwell, J. R. (1999) *J. Appl. Cryst.* **32**, 554–562.
- Collaborative Computational Project, Number 4 (1994) *Acta Crystallogr. D* **50**, 760–763.
- Berman, H. M., Westbrook, J. Z., Gilliland, G., Bhat, T. N., Weissig, H., Shindyalov, I. N. & Bourne, P. E. (2000) *Nucleic Acids Res.* **28**, 235–242.
- McRee, D. E. (1999) *J. Struct. Biol.* **125**, 156–165.
- Sheldrick, G. M. (1990) *Acta Crystallogr. A* **46**, 467–473.